Analysis of magnetic saturation effects in the squirrel cage induction generators

Redouane Hachelaf[1,2], Djilali Kouchih[1], Mohamed Tadjine[2], Mohamed Seghir Boucherit[2]

[1]Automatic and Electrotechnic Department, University Blida 1, Blida, Algeria
[2]Automatic Control Department, National Polytechnics School, Algiers, Algeria

Article Info	ABSTRACT
	This work concerns an investigation on the analysis of the magnetic saturation effects in the three-phase squirrel cage induction generator which is considered as a main device in wind energy conversion systems. The magnetic saturation is considered as an important factor causing destructive effects on power qualities such as harmonics and distortion. Several approaches have been presented in the literature for the modeling of the electric machines considering magnetic saturation. The widely used and precise approach is the finite elements method which is particularly characterized by its high computational time. The novelty in this paper is that a state model has been developed for the healthy conditions of the three-phase squirrel cage induction generators considering the experimental variation of the magnetizing inductance in terms of the magnetizing current. Simulation and experimental tests are provided to extract some important signatures on stator voltages and currents. It will be deduced that the spectrum analysis of stator currents contains useful information on magnetic saturation. Experimental and theoretical results illustrate the consistency of this approach for the modeling and analysis of the squirrel cage induction generators considering the magnetic saturation. *This is an open access article under the <u>CC BY-SA</u> license.*

Corresponding Author:

Redouane Hachelaf
Automatic and Electrotechnic Department, University Blida 1
Blida, 09000, Algeria
Email: haclefr@yahoo.fr

1. INTRODUCTION

Alternative current (AC) generators are considered as the main electrical energy sources particularly for high power systems. Power qualities such as stability, harmonics, and distortion are the main criteria of such energy sources. These qualities must be discussed particularly in induction generators which are recently considered as the main device in wind energy conversion systems due to their robust construction, low-cost maintenance and no separate excitation system [1]–[6]. From different factors having destructive effects on power qualities, magnetic saturation is considered as an important factor causing harmonic components through stator voltages and currents. It has been shown that the magnetic saturation produces destructive effects on performances of AC machines. The most effects are noise, increased losses and reduced insulation life [7]–[12]. In addition, the magnetic saturation causes the variation of machine inductances in terms of magnetizing current.

Analysis of magnetic saturation in AC machines becomes an important topic of research and particularly attention is given to the modeling of magnetic saturation in induction machines. For this purpose, Roshandel *et al.* [13] investigated the use of subdomain technique to predict performance of the induction machine considering saturation effects. Mölsä *et al.* [14] proposed a dynamic model for saturated induction

machines with closed rotor slots and deep bars. Fatima *et al.* [15] investigate the use of an improved permeance-based equivalent circuit model considering the frequency and magnetic curve dependent core loss branches for the prediction of the electromagnetic performances of induction machines. Mollaeian *et al.* [16] use fourier-based modeling of an induction machine considering the finite permeability and nonlinear magnetic properties. Ojaghi and Nashari [17] investigate the modeling of eccentric squirrel-cage induction motors with slotting effect and saturable teeth reluctances. Amiri *et al.* [18], Moreira and Lipo [19] investigate the modeling of saturated alternative current machines including air gap flux harmonic components. From several methods, the widely used is the finite elements method (FEM) [20]–[22]. This method is particularly characterized by the fact it gives good results, but its major inconvenience is the high computational time. The contribution of this work is that a state model has been developed for the healthy conditions of the squirrel cage induction generators (SCIG) considering the variation of machine inductances under the magnetic saturation. For this purpose, the machine inductances are calculated in terms of the magnetizing current. This approach is based on the assumption that both stator and rotor windings are replaced by an equivalent sinusoidally distributed windings [23], [24]. All the rotor variables are referred to the stator windings and called the equivalent variables. The rotor equivalent parameters are predicted in terms of the actual rotor bar resistances and inductances.

To characterize the magnetic saturation effects in the SCIG, we are interested to the classical spectrum analysis due to its inherent advantages. This analysis is applied on stator currents, fluxes, and voltages. Experimental and theoretical results illustrate the consistency of this approach for the modeling and analysis of the magnetic saturation in the SCIG.

2. SCIG EQUATIONS

2.1. Stator voltage equations

The direction of stator current is indicated by Figure 1. So, the stator voltage equation is expressed by (1). With the convention of the positive direction of stator and rotor currents, the stator flux becomes as given by (2).

$$\frac{d[\Phi_s]}{dt} = [R_s][i_s] + [v_n]$$

$$[\Phi_s] = [\Phi_{as}\ \Phi_{bs}\ \Phi_{cs}]^T \tag{1}$$

$$[\Phi_s] = -[L_{ss}][i_s] - [L_{sr}]_i[i_r] \tag{2}$$

The matrix of the stator inductances is expressed by (3).

$$[L_{ss}] = \begin{bmatrix} L_{ms} + L_{ls} & -L_{ms}/2 & -L_{ms}/2 \\ -L_{ms}/2 & L_{ms} + L_{ls} & -L_{ms}/2 \\ -L_{ms}/2 & -L_{ms}/2 & L_{ms} + L_{ls} \end{bmatrix} \tag{3}$$

L_{ms} is the stator magnetizing inductance; and L_{ls} is the stator leakage inductance. The magnetizing inductance is given by (4).

$$L_{ms} = \frac{2}{3}L_m \tag{4}$$

L_m is the magnetizing inductance. Based on Kirchhoff laws, the stator and capacitor currents are expressed by (5) and (6) respectively.

$$[i_{sd}] = [i_c] + [i_l] \tag{5}$$

$$[i_c] = C\frac{d[v_n]}{d_t} \tag{6}$$

For resistive load, the load current is given by (7).

$$[i_l] = [R_l]^{-1}[v_n] \tag{7}$$

C is the excitation capacitor. Z_a, Z_b, and Z_c are the load impedances.
The matrix of load resistances is expressed by (8).

$$[Rl] = \begin{bmatrix} rl & 0 & 0 \\ 0 & rl & 0 \\ 0 & 0 & rl \end{bmatrix} \tag{8}$$

So, the derivative of the vector of stator voltage is given by (9).

$$\frac{d[v_n]}{dt} = \frac{1}{C}([i_s] - [R_l]^{-1}[v_n]) \tag{9}$$

$$[v_n] = [v_{an}\ v_{bn}\ v_{cn}]^T$$
$$[i_s] = [i_{as}\ i_{bs}\ i_{cs}]^T$$

v_{an}, v_{bn}, and v_{cn} are the phase voltages referred to the neutral point 'n'. i_{as}, i_{bs}, and i_{cs} are the line currents.

$$[i_c] = [i_{ac}\ i_{bc}\ i_{cc}]^T$$
$$[i_l] = [i_{al}\ i_{bl}\ i_{cl}]^T$$

i_{ac}, i_{bc}, and i_{cc} are the currents in the capacitors. i_{al}, i_{bl}, and i_{cl} are the load currents. R_l is the load resistance.
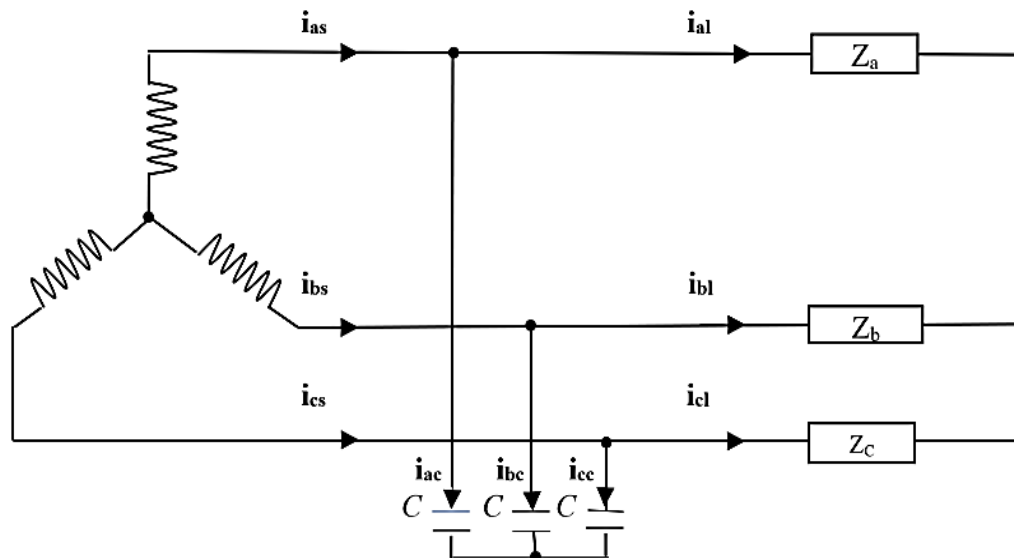

Figure 1. Squirrel cage induction generator (SCIG) [24]

2.2. Rotor voltage equations

The squirrel cage rotor can be approximated as three identical windings. When expressing the rotor voltage equations, all rotor variables are referred to the stator windings and called the equivalent variables. With the convention of the positive direction of stator and rotor currents, the rotor voltage equation is expressed by (10).

$$\frac{d[\Phi_r]}{dt} = [R_r][i_r] \tag{10}$$

The rotor flux vector is expressed by (11).

$$[\Phi_r] = -[L_{rs}][i_s] - [L_{rr}][i_r] \tag{11}$$

The matrix of the equivalent rotor-stator mutual inductances is defined by (12).

$$[L_{rs}] = [L_{sr}]^T \tag{12}$$

$[i_r]$ is the vector of equivalent rotor currents; $[R_r]$ is the matrix of the equivalent rotor resistances; $[L_{rs}]$ is the matrix of the equivalent rotor-stator mutual inductances; $[L_{rr}]$ is the matrix of the equivalent rotor inductances. The matrices of the equivalent stator-rotor mutual inductances and rotor resistances are defined by (13) and (14) respectively.

$$[L_{sr}] = L_{ms} \begin{bmatrix} cos(\theta) & cos(\theta - \frac{2\pi}{3}) & cos(\theta + \frac{2\pi}{3}) \\ cos(\theta + \frac{2\pi}{3}) & cos(\theta) & cos(\theta - \frac{2\pi}{3}) \\ cos(\theta - \frac{2\pi}{3}) & cos(\theta - \frac{2\pi}{3}) & cos(\theta) \end{bmatrix} \tag{13}$$

$$[R_r] = r_r \begin{bmatrix} 1 & 0 & 0 \\ 0 & 1 & 0 \\ 0 & 0 & 1 \end{bmatrix} \tag{14}$$

For the matrix of equivalent rotor inductances, it's expressed by (15).

$$[L_{rr}] = \begin{bmatrix} L_{ms} + L_{lr} & -{L_{ms}}/{2} & -{L_{ms}}/{2} \\ -{L_{ms}}/{2} & L_{ms} + L_{lrr} & -{L_{ms}}/{2} \\ -{L_{ms}}/{2} & -{L_{ms}}/{2} & L_{ms} + L_{lr} \end{bmatrix} \tag{15}$$

It can be demonstrated that the equivalent rotor resistance and leakage inductance can be calculated using (16)-(18) [23].

$$r_r = \left(\frac{3\pi}{8}\right) \frac{N_s^2}{n_b sin^2(\delta)} [rb(1 - cos(\alpha_r)) + re] \tag{16}$$

$$L_{lr} = \frac{6}{nb} \left(\frac{\pi}{4}\right)^2 N_s^2 \left[2l_b + \frac{le}{sin^2\delta}\right] + \frac{3}{2} L_{ms} \left[\frac{\delta^2}{sin^2\delta} - 1\right] \tag{17}$$

$$\delta = \frac{\alpha_r}{2} \tag{18}$$

2.3. Calculation of machine currents

To calculate the machine currents, it is convenient to determine the two components ias and ibs. The vector of the stator currents can be calculated using (19) to (21).

$$[i_s] = [B_s][i_{abs}] \tag{19}$$

With:

$$[B_s] = \begin{bmatrix} +1 & 0 \\ 0 & +1 \\ -1 & -1 \end{bmatrix} \tag{20}$$

$$[i_{abs}] = \begin{bmatrix} i_{as} \\ i_{bs} \end{bmatrix} \tag{21}$$

Using two independent components, we define the flux vector by (22).

$$[\Phi_{abs}] = [A_s][\Phi_s] \tag{22}$$

With the convention of the positive direction of stator and rotor currents, we can verify that the stator and rotor fluxes are calculated using (23) to (28).

$$[\Phi_{abs}] = -[L_{sd}][i_{abs}] - [L_{srd}][i_r] \tag{23}$$

$$[\Phi_r] = -[L_{rsd}][i_{abs}] - [L_{rr}][i_r] \tag{24}$$

With,

$$[A_s] = \begin{bmatrix} 1 & -1 & 0 \\ 0 & 1 & -1 \end{bmatrix} \tag{25}$$

$$[L_{sd}] = [A_s][L_{ss}][B_{sd}] \tag{26}$$

$$[L_{srd}] = [A_s][L_{sr}] \tag{27}$$

$$[L_{rsd}] = [L_{rs}][B_s] \tag{28}$$

Using (23) and (24), we get (29) and (30).

$$[i_{abs}] = -([L_{sd}] - [L_{srd}][L_{rr}]^{-1}[L_{rsd}])^{-1}([\Phi_{abs}] - [L_{srd}][L_{rr}]^{-1}[\Phi_r]) \tag{29}$$

$$[i_r] = -([L_{rr}] - [L_{rsd}][L_{sd}]^{-1}[L_{srd}])^{-1}([\Phi_r] - [L_{rsd}][L_{sd}]^{-1}[\Phi_{abs}]) \tag{30}$$

2.4. SCIG state model

Using (1), (9), (10), (29), and (30), the state model of SCIG is illustrated by (31).

$$\begin{cases} \frac{d[\Phi_s]}{dt} = -[R_s][B_s]([L_{sd}] - [L_{srd}][L_{rr}]^{-1}[L_{rsd}])^{-1}([\Phi_{abs}] - [L_{srd}][L_{rr}]^{-1}[\Phi_r]) + [v_n] \\ \frac{d[\Phi_r]}{dt} = -[R_r]([L_{rr}] - [L_{rsd}][L_{sd}]^{-1}[L_{srd}])([\Phi_r] - [L_{rsd}][L_{sd}]^{-1}[\Phi_{abs}]) \\ \frac{d[v_n]}{dt} = \frac{1}{C}([T][B_s][C_s]([\Phi_{abs}] - [L_{srd}][L_{rr}]^{-1}[\Phi_r]) - [R_l]^{-1}[v_n]) \\ J\frac{d\Omega}{dt} = T_m - T_e - f_v\Omega \end{cases} \tag{31}$$

Where J is the inertia of the rotor and the connected load, T_e is the electromagnetic torque, T_m is the motorized torque, Ω the mechanical angular speed and fv is the viscose friction coefficient. The electromagnetic torque is expressed by (32) [25].

$$T_e = \frac{P}{2}[i_s]^t \frac{\partial[L_{sr}]}{\partial\theta}[i_r] \tag{32}$$

P is the number of poles pairs and θ is the electrical angular displacement of the rotor.

3. SIMULATION RESULTS

Using the MATLAB environment, the above state model is simulated for a SCIG of 4 kW, 220/ 380 V – 50 Hz. The excitation capacitor is C = 50 µF. A starting up with no load is considered. At time t = 2.5 s, a balanced load of resistance 125 Ω is supplied by the SCIG. The SCIG is rotated at mechanical speed of 3050 tr/mn imposing fundamental frequency of 50 Hz for the stator voltages and currents. The stator voltage and its spectrum analysis are illustrated by Figures 2(a) and 2(b), respectively. The stator flux, their hodograph and spectrum analysis are shown by Figures 2(c)-2(e), respectively. The spectrum analysis of the stator current is illustrated by Figure 2(f).

As results of magnetic saturation effects, specific harmonics of order 2k+1 with k an integer (150 Hz, 250 Hz, 350 Hz, and 450 Hz…) are observed through the spectrum analysis of the stator voltages, fluxes, and currents as mentioned by Figures 2(b), 2(e), and 2(f). These harmonics explain the destructive effect of magnetic saturation such as noise, increase losses, reduced insulation life. As illustrated by Figure 2(a), Figure 2(c), and Figure 2(d), the temporary characteristics of the stator voltage, flux and the circular form of the stator flux are explained by the fact that the SCIG operate in balanced conditions.
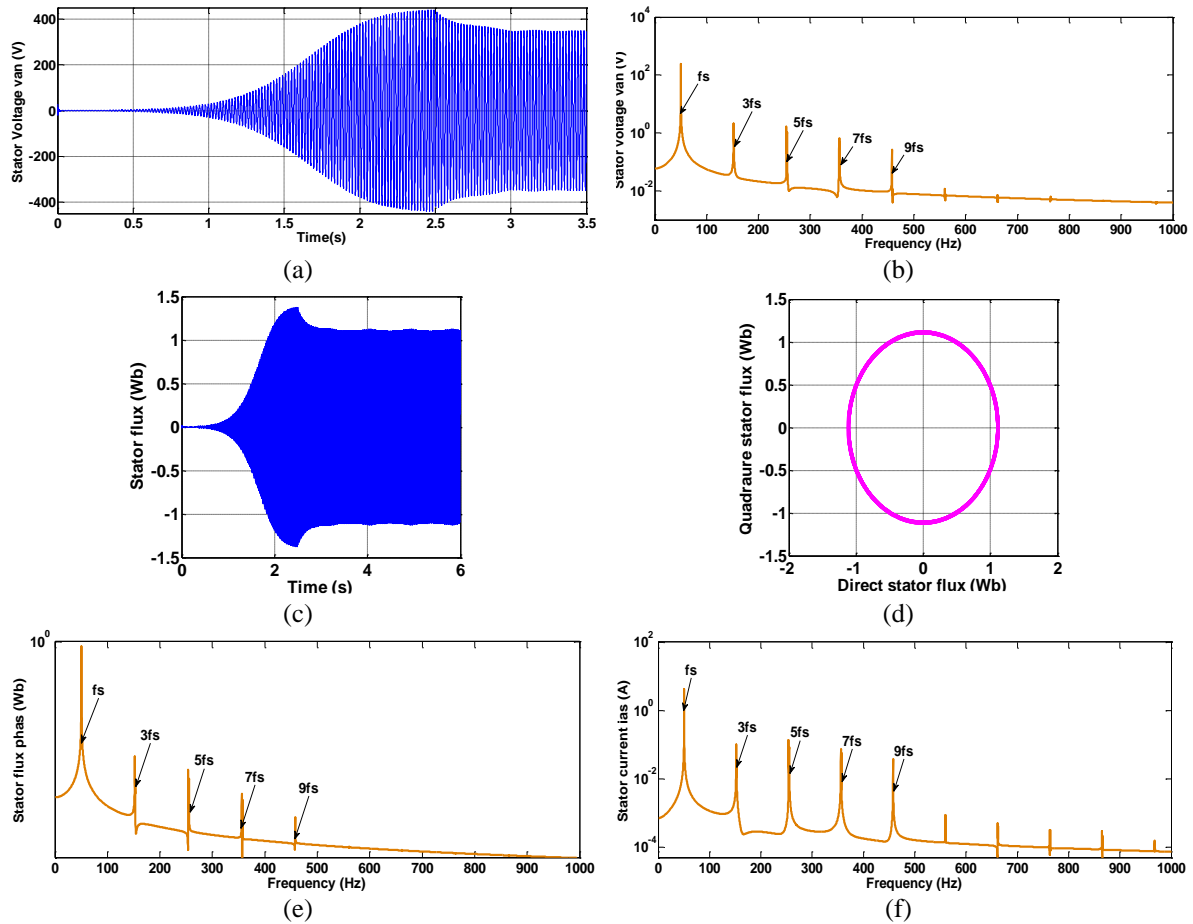
Figure 2. Simulation results of SCIG: (a) stator voltage v_{an} [24], (b) spectrum analysis of stator voltage v_{an}, (c) stator flux phas [24], (d) hodograph of stator fluxes, (e) spectrum analysis of stator flux phas, and (f) spectrum analysis of stator current i_{as}

4. EXPERIMENTAL STUDY

4.1. Magnetizing inductance

To validate the theoretical study, an experimental test has been conducted on the three phase SCIG of 4 kW, 220/380 V – 50 Hz. The magnetizing inductance has been identified experimentally and expressed in terms of magnetizing current using an approximate function. For this purpose, the SCIG is coupled with a synchronous motor and a variable voltage is applied on the stator windings to measure the effective value of magnetizing flux in terms of the magnetizing current. Then, the magnetizing inductance is illustrated by Figure 3. In the literature, some functions have been proposed to approximate the magnetizing inductance in terms of the magnetizing current. In this study, it is approximated as indicated by (33).

$$L_m = \frac{arctan(0.9 i_m)}{2 i_m} \tag{33}$$

4.2. Validation of the theoretical study

To validate the theoretical study, an experimental test has been conducted on the three phase SCIG of 4 kW, 220/380 V – 50 Hz. The excitation capacitor is $C = 50\ \mu F$. The SCIG is rotated at mechanical speed of 3050 tr/mn imposing fundamental frequency of 50 Hz for the stator voltages. A starting up with no load is considered and followed by the applying of balanced load of resistance 125 Ω. The stator currents are measured using shunt resistors. The stator voltage and its spectrum analysis are illustrated by Figure 4(a) and Figure 4(b) respectively.

It is important to note that the magnetizing inductance is sensitive to the magnetizing current depending on the load conditions. Figure 4(a) shows the temporary characteristic of the stator voltage which depends on the mechanical speed and the load conditions. Concerning Figure 4(b), it illustrates the presence of the harmonics (150 Hz, 250 Hz, 350 Hz…) through stator voltage. Systematically, these harmonics will be

reproduced through the stator currents and fluxes. These harmonic components will generate destructive effects such as noise, excessive heating and reduce insulation life of the SCIG.
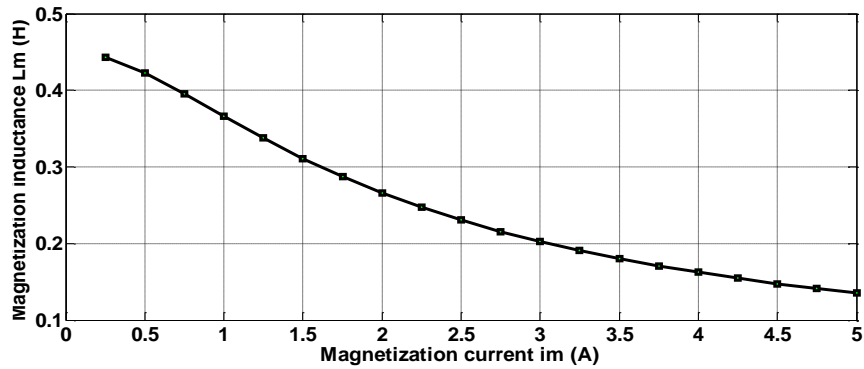

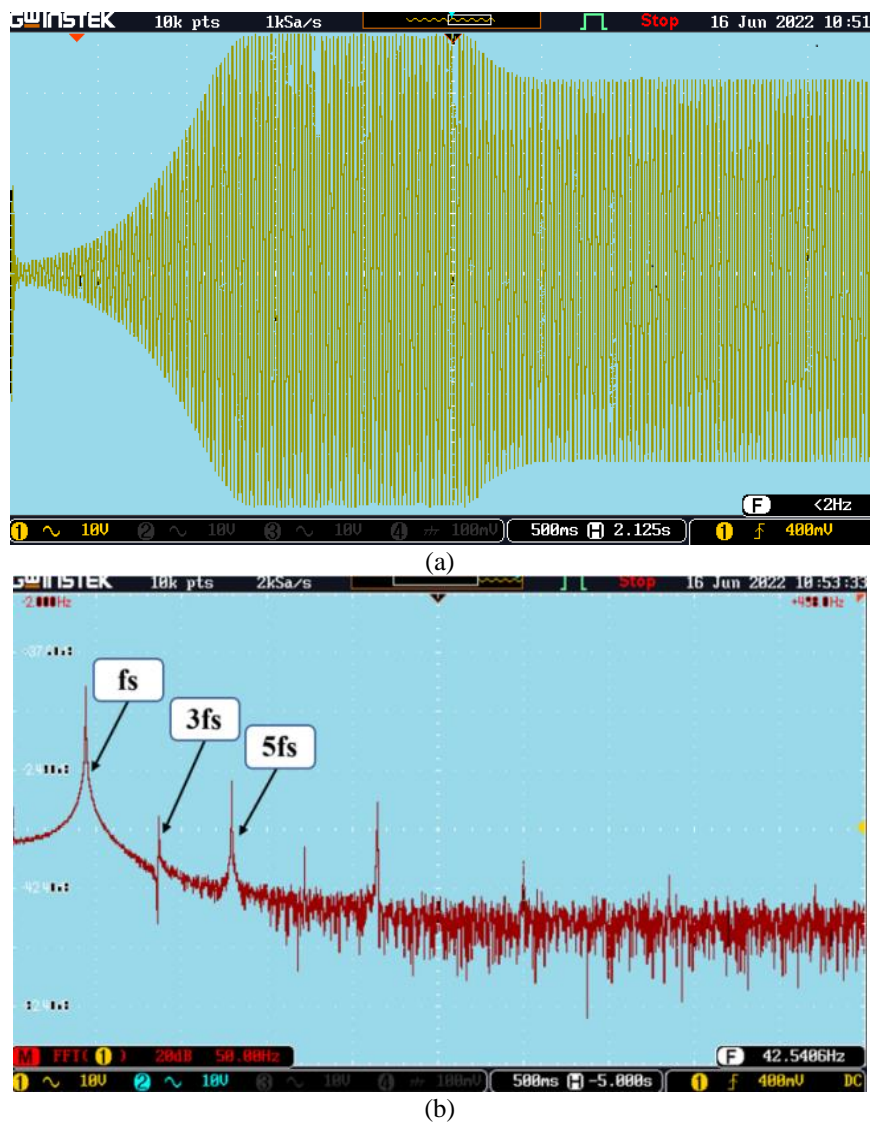Figure 3. Magnetizing inductance L_m

(a)

(b)

Figure 4. Experimental results of SCIG: (a) stator voltage v_{an} [24] and
(b) spectrum analysis of stator voltage v_{an}

5.   CONCLUSION

An analytical approach for the modeling and analysis of SCIG considering magnetic saturation has been synthetized and experimentally validated. The comparison of experimental and simulation results shows that harmonic components of the stator currents are produced due to the magnetic saturation. Using this approach, various characteristics are analyzed such as stator voltages and currents. This work must be performed by a future work to clearly discriminate the magnetic saturation from other stator asymmetries where all cases exhibit similar kind of current and flux signatures.

REFERENCES

[1]   R. Mahroug, M. Matallah, and S. Abudura, "Modeling of wind turbine based on dual DFIG generators," *International Journal of Power Electronics and Drive Systems*, vol. 13, no. 2, pp. 1170–1185, 2022, doi: 10.11591/ijpeds.v13.i2.pp1170-1185.
[2]   A. Athamneh and B. Al Majali, "Voltage stability enhancement for large scale squirrel cage induction generator based wind turbine using STATCOM," *International Journal of Power Electronics and Drive Systems (IJPEDS)*, vol. 12, no. 3, pp. 1784–1794, Sep. 2021, doi: 10.11591/ijpeds.v12.i3.pp1784-1794.
[3]   W. E. Vanco, F. B. Silva, J. R. B. A. Monteiro, C. M. R. De Oliveira, and L. C. Gomes, "Theoretical-experimental analysis of the induction generator in the use of distributed generation," *IEEE Latin America Transactions*, vol. 19, no. 3, pp. 396–403, Mar. 2021, doi: 10.1109/TLA.2021.9447688.
[4]   K. Nagarajan and A. J. G. David, "Self-excited asynchronous generator with PV array in detained autonomous generation systems," *International Journal of Power Electronics and Drive Systems*, vol. 14, no. 1, pp. 358–368, 2023, doi: 10.11591/ijpeds.v14.i1.pp358-368.
[5]   X. Jin, Z. Xu, and W. Qiao, "Condition monitoring of wind turbine generators using SCADA data analysis," *IEEE Transactions on Sustainable Energy*, vol. 12, no. 1, pp. 202–210, Jan. 2021, doi: 10.1109/TSTE.2020.2989220.
[6]   E. O. Silva, W. E. Vanco, and G. C. Guimaraes, "Capacitor Bank Sizing for Squirrel Cage Induction Generators Operating in Distributed Systems," *IEEE Access*, vol. 8, pp. 27507–27515, 2020, doi: 10.1109/ACCESS.2020.2971704.
[7]   R. T. Novotnak, J. Chiasson, and M. Bodson, "High-performance motion control of an induction motor with magnetic saturation," *IEEE Transactions on Control Systems Technology*, vol. 7, no. 3, pp. 315–327, May 1999, doi: 10.1109/87.761052.
[8]   H. T. Eickhoff, R. Seebacher, and A. Muetze, "Space harmonics and saturation interaction in fault-tolerant induction machine drives due to a zero-sequence stator current," *IEEE Transactions on Industry Applications*, vol. 57, no. 5, pp. 4958–4969, Sep. 2021, doi: 10.1109/TIA.2021.3095833.
[9]   A. Yahiaoui and F. Bouillault, "Saturation effect on the electromagnetic behaviour of an induction machine," *IEEE Transactions on Magnetics*, vol. 31, no. 3, pp. 2036–2039, May 1995, doi: 10.1109/20.376443.
[10]   J. E. Brown, K. Kovacs, and P. Vas, "A method of including the effects of main flux path saturation in the generalized equations of A.C. machines," *IEEE Transactions on Power Apparatus and Systems*, vol. PAS-102, no. 1, pp. 96–103, Jan. 1983, doi: 10.1109/TPAS.1983.318003.
[11]   M. Es-Semyhy, A. Ba-Razzouk, M. El Haroussi, and M. Madark, "Nonlinear control of an induction motor taking into account saturation and rotor resistance variation effects," *International Journal of Power Electronics and Drive Systems (IJPEDS)*, vol. 14, no. 1, pp. 60–76, Mar. 2023, doi: 10.11591/ijpeds.v14.i1.pp60-76.
[12]   R. Nazir, S. Syafii, A. Pawawoi, F. Akbar, and Y. Arfan, "Effect analysis of residual magnetism availability level on the success of voltage generation processes in self-excited induction generators," *International Journal of Power Electronics and Drive Systems (IJPEDS)*, vol. 11, no. 3, pp. 1211–1219, Sep. 2020, doi: 10.11591/ijpeds.v11.i3.pp1211-1219.
[13]   E. Roshandel, A. Mahmoudi, S. Kahourzade, and W. L. Soong, "Saturation consideration in modeling of the induction machine using subdomain technique to predict performance," *IEEE Transactions on Industry Applications*, vol. 58, no. 1, pp. 261–272, Jan. 2022, doi: 10.1109/TIA.2021.3125915.
[14]   E. Molsa, S. E. Saarakkala, M. Hinkkanen, A. Arkkio, and M. Routimo, "A dynamic model for saturated induction machines with closed rotor slots and deep bars," *IEEE Transactions on Energy Conversion*, vol. 35, no. 1, pp. 157–165, Mar. 2020, doi: 10.1109/TEC.2019.2950810.
[15]   A. Fatima *et al.*, "Electromagnetic Performance Prediction of an Induction Machine Using an Improved Permeance-Based Equivalent Circuit Model Considering the Frequency and B-H Curve Dependent Core Loss Branches," *IEEE Transactions on Industry Applications*, vol. 59, no. 2, pp. 1283–1294, 2023, doi: 10.1109/TIA.2022.3200350.
[16]   A. Mollaeian *et al.*, "Fourier-Based Modeling of an Induction Machine Considering the Finite Permeability and Nonlinear Magnetic Properties," *IEEE Transactions on Energy Conversion*, vol. 36, no. 4, pp. 3427–3437, 2021, doi: 10.1109/TEC.2021.3085748.
[17]   M. Ojaghi and S. Nasiri, "Modeling eccentric squirrel-cage induction motors with slotting effect and saturable teeth reluctances," *IEEE Transactions on Energy Conversion*, vol. 29, no. 3, pp. 619–627, 2014, doi: 10.1109/TEC.2014.2320823.
[18]   N. Amiri, S. Ebrahimi, and J. Jatskevich, "Induction Machine Modeling Considering Magnetizing Flux Saturation With Air-Gap Harmonics," *IEEE Transactions on Energy Conversion*, vol. 36, no. 4, pp. 3376–3386, Dec. 2021, doi: 10.1109/TEC.2021.3080667.
[19]   J. C. Moreira and T. A. Lipo, "Modeling of Saturated ac Machines Including Air Gap Flux Harmonic Components," *IEEE Transactions on Industry Applications*, vol. 28, no. 2, pp. 343–349, 1992, doi: 10.1109/28.126740.
[20]   T. Lubin, T. Hamiti, H. Razik, and A. Rezzoug, "Comparison Between Finite-Element Analysis and Winding Function Theory for Inductances and Torque Calculation of a Synchronous Reluctance Machine," *IEEE Transactions on Magnetics*, vol. 43, no. 8, pp. 3406–3410, Aug. 2007, doi: 10.1109/TMAG.2007.900404.
[21]   R. De Weerdt, E. Tuinman, K. Hameyer, and R. Belmans, "Finite element analysis of steady state behavior of squirrel cage induction motors compared with measurements," *IEEE Transactions on Magnetics*, vol. 33, no. 2 PART 2, pp. 2093–2096, 1997, doi: 10.1109/20.582733.
[22]   Y. Du Terrail, J. C. Sabonnadiere, P. Masse, and J. L. Coulomb, "Nonlinear Complex Finite Elements Analysis of Electromagnetic Field in Steady-State AC Devices," *IEEE Transactions on Magnetics*, vol. 20, no. 4, pp. 549–552, 1984, doi: 10.1109/TMAG.1984.1063125.
[23]   A. R. Munoz and T. A. Lipo, "Complex vector model of the squirrel-cage induction machine including instantaneous rotor bar currents," *IEEE Transactions on Industry Applications*, vol. 35, no. 6, pp. 1332–1340, 1999, doi: 10.1109/28.806047.

[24] D. Kouchih and H. Redouane, "Theoretical and Experimental Analysis of the Squirrel Cage Induction Generators Operating under Unbalanced Conditions Theoretical and Experimental Analysis of the Squirrel Cage Induction Generators Operating under Unbalanced Conditions," *Research Square*, pp. 0–12, 2022, doi: 10.21203/rs.3.rs-2347428/v1.

[25] P. C. Krause, *Analysis of Electric Machinery*. McGraw-Hill Book Company, 1987.

BIOGRAPHIES OF AUTHORS

Redouane Hachelaf iD 8 SC ◐ is an assistant professor in automatic and electrotechnics Department at the University Blida 1, Algeria. He received the engineer degree from the University of Medea in 2008, the magister degree from the Military Polytechnics School, Bordj El Bahri, Algeria in 2011. Currently, he is Ph.D. student in automatic control at the National Polytechnics School, Algiers, Algeria. He can be contacted at email: haclefr@yahoo.fr.

Djilali Kouchih iD 8 SC ◐ is an associate professor in Automatic and Electrotechnics Department at the University Blida 1, Algeria. He received the engineer degree, the Ph.D. degree in electrical engineering from the National Polytechnics School, of Algiers, Algeria, in 1994, and 2015 respectively. His research interests are in the area of electrical drives, process control, diagnosis, and renewable energies. He can be contacted at email: djkouchih@yahoo.fr.

Mohamed Tadjine iD 8 SC ◐ is with the Department of Automatic Control at the National Polytechnics School of Algiers, Algeria, where he is currently professor. He received the engineering degree from the National Polytechnic of Algiers, Algeria, in 1990 and the Ph.D. degree in automatic control from the national polytechnic institute of Grenoble (INPG), France in 1994. From 1995 to 1997, he was a researcher at the automatic systems laboratory, Amiens, France. His main research areas are:nonlinear and robust control, observer design, fault detection and fault tolerant control, robotics, and electrical drives and quantum computing. He can be contacted at email: tadjine@yahoo.fr.

Mohamed Seghir Boucherit iD 8 SC ◐ is a professor, head of Industrial Systems and Diagnosis Team of the Process Control Laboratory in the Department of Automatic Control the National Polytechnics School, Algiers, Algeria.He received the engineer degree in electrotechnics, the magister degree and the Ph.D. degree in electrical engineering, from the National Polytechnics School, Algiers, Algeria, in 1980, 1988 and 1995 respectively. His research interests are in the area of electrical drives, process control, and diagnosis. He can be contacted at email: ms_boucherit@yahoo.fr.